'Direction of Arrival' Estimation Algorithm: Direction Lock Loop

Seunghyun Min, Kwang Bok Lee, and Yong-Hwan Lee
School of Electrical Engineering, Seoul National University
Shinlim-dong, Kwanak-gu, Seoul 151-742, Korea
TEL: +82-2-880-8415 FAX: +82-2-880-8215
E-mail: shmin@mobile.snu.ac.kr, klee@snu.ac.kr, ylee@snu.ac.kr

***Abstract*- In this paper, a new direction of arrival (DOA) estimation algorithm, direction lock loop (DiLL), is proposed. It has a similar concept to the delay lock loop (DLL) that is used for synchronization. It estimates the DOA of a signal by iterations, and can track the DOA of a moving source. The DiLL scheme is found to track better than the DOA estimation scheme based on the PASTd, and its performance is less sensitive to the DOA of a signal than that of the DOA estimation scheme based on the PASTd. The DOA estimation accuracy and the tracking capability are demonstrated by analysis and computer simulations.**

I. INTRODUCTION

The demand for wireless communication services is growing at an explosive rate. To enhance the capacity of wireless communication systems, space division multiple access (SDMA) systems are of considerable interest. The SDMA systems are implemented by using smart antenna systems. In recent years, smart antenna systems based on direction of arrival (DOA) estimation methods have been developed. The problem of estimating the DOA of signals from array data is well documented in [1]. Eigen structure methods such as MUSIC and ESPRIT have been found widespread use in providing estimates of the DOA of signals [2], [3]. However, the computational burden of the eigen analysis increases significantly with the number of antenna elements.

To reduce the complexity of the eigen methods, projection approximation subspace tracking with deflation (PASTd) was proposed by Yang [4], [5]. This algorithm tracks the signal subspace recursively. Using this algorithm, the eigenvectors may be tracked easily. However, the PASTd algorithm is not for DOA estimation but for signal subspace estimation. Thus, an additional DOA estimation algorithm such as MUSIC or ESPRIT, is required to estimate the DOA of signals.

In this paper, a new DOA estimation algorithm is proposed. Since this algorithm is similar to the delay lock loop (DLL) used for synchronization [6], it is referred to as the direction lock loop (DiLL) scheme in this paper. An error signal for DOA estimation is generated from the correlation of an input signal and the array response vectors whose directions are $\pm\Delta\theta$ shifted from the DOA estimate. This error signal is used to update DOA estimates iteratively. The DiLL does not require a separate DOA estimation. Thus, the DiLL scheme is conceptually simple, and tracks a moving source by iterations.

This paper is organized as follows. The system model is shown in Section II. In Section III, the new DOA estimation scheme, DiLL is presented and the characteristics of the DiLL scheme are explained. The performance analysis of the DiLL scheme is shown in Section IV. In Section V, numerical results are given. Conclusions are drawn in Section VI.

II. SYSTEM MODEL

Consider a uniform linear array with N half-wavelength spacing antenna elements. For simplicity of explanation, the single user case is investigated in this paper. Thus, the received signal may be represented as

$$\mathbf{r}(t) = \mathbf{a}(\theta)d(t) + \mathbf{v}(t) \tag{1}$$

where

- $\mathbf{r}(t) = [r_1(t), \ \cdots, \ r_N(t)]^T$ is an $N\times 1$ vector of received signals at time t;
- $\mathbf{a}(\theta)$ is the array response vector for a signal with a DOA θ. The value of θ is constant when the source is fixed, or varies when the source is moving. The vector $\mathbf{a}(\theta)$ is defined as
  $\mathbf{a}(\theta) = \left[e^{j0} \quad e^{j\pi\sin\theta} \quad \cdots \quad e^{j(N-1)\pi\sin\theta}\right]^{\mathrm{T}}$;
- $d(t)$ is a source signal at time t, and it is assumed $|d(t)|^2 = 1$ for simplicity of explanation;
- $\mathbf{v}(t)$ is an $N\times 1$ additive noise vector, which is assumed to be spatially and temporally white, having Gaussian distribution with covariance matrix $\sigma^2\mathbf{I}$, where σ^2 is the noise variance.

III. DIRECTION LOCK LOOP (DILL)

A. Principles of the DiLL Scheme

In this subsection, the principle of the DiLL scheme is explained. Fig. 1 shows a block diagram of the DiLL scheme. Note that its structure is similar to the DLL for time-domain synchronization. The received signal vector is correlated simultaneously with right-shifted and left-shifted array response vectors $\mathbf{a}(\hat{\theta}(i)+\Delta\theta)$ and $\mathbf{a}(\hat{\theta}(i)-\Delta\theta)$ to produce correlator outputs $z_R(i)$ and $z_L(i)$, when the DOA estimate at the ith time is $\hat{\theta}(i)$ and the shift angle is $\Delta\theta$ which is set to a constant value regardless of θ, for simplicity of explanation. The correlator outputs $z_R(i)$ and $z_L(i)$ may be represented as

$$z_R(i) = \frac{1}{N}\mathbf{a}^H(\hat{\theta}(i)+\Delta\theta)\mathbf{r}(i) = d(i)R(\theta,\hat{\theta}(i)+\Delta\theta) + v_R(i)$$
$$z_L(i) = \frac{1}{N}\mathbf{a}^H(\hat{\theta}(i)-\Delta\theta)\mathbf{r}(i) = d(i)R(\theta,\hat{\theta}(i)-\Delta\theta) + v_L(i) \tag{2}$$

where $R(\theta_1,\theta_2)$ is a normalized spatial correlation function, which is defined as

$$R(\theta_1,\theta_2) = \frac{1}{N}\mathbf{a}^H(\theta_2)\mathbf{a}(\theta_1) = \frac{1}{N}\sum_{n=1}^{N} e^{j\pi(n-1)(\sin\theta_1-\sin\theta_2)}, \tag{3}$$

$v_R(i) = \frac{1}{N}\mathbf{a}^H(\hat{\theta}(i)+\Delta\theta)\mathbf{v}(i)$, $v_L(i) = \frac{1}{N}\mathbf{a}^H(\hat{\theta}(i)-\Delta\theta)\mathbf{v}(i)$, and the superscript H denotes the Hermitian transpose.

The difference between the amplitude-squares of two correlator outputs is used to produce an error signal $e(i)$, which is defined as

$$e(i) = |z_R(i)|^2 - |z_L(i)|^2 = G(\hat{\theta}(i)|\theta) + v_e(i) \tag{4}$$

where $G(\hat{\theta}(i)|\theta)$ is a direction discriminator characteristic and is defined as

$$G(\hat{\theta}(i)|\theta) = |R(\theta, \hat{\theta}(i) + \Delta\theta)|^2 - |R(\theta, \hat{\theta}(i) - \Delta\theta)|^2 \tag{5}$$

and $v_e(i)$ is defined as

$$\begin{aligned} v_e(i) &= |v_R(i)|^2 - |v_L(i)|^2 \\ &+ 2\,\mathrm{Re}\{d(i)(R(\theta, \hat{\theta}(i) + \Delta\theta)v_R^*(i) - R(\theta, \hat{\theta}(i) - \Delta\theta)v_L^*(i))\} \end{aligned}. \tag{6}$$

The characteristics of $G(\hat{\theta}(i)|\theta)$ determine the DOA estimation performance of the DiLL and the plot of $G(\hat{\theta}(i)|\theta)$ is referred to the S-curve. The error signal, $e(i)$ is filtered and fed to the numerically controlled oscillator (NCO) to update DOA estimates iteratively. Hence, the DOA estimate at the $(i+1)$th time may be expressed as

$$\hat{\theta}(i+1) = \hat{\theta}(i) + K_0 \cdot (e(i) \otimes f(i)) \tag{7}$$

where $f(i)$ is the impulse response of the loop filter, K_0 is the NCO gain, and $\otimes$ denotes convolution.

Fig. 2 shows the plot of $G(\hat{\theta}|\theta)$ as a function of $\hat{\theta}$, using (5), when $\theta = 0^\circ$, N=4, and $\Delta\theta$=12.24°. When the DOA estimate at the ith time $\hat{\theta}(i)$ is less than the actual DOA θ, the error signal is larger than zero, and thus NCO increases the DOA estimate value at the $(i+1)$th time. When $\hat{\theta}(i)$ is larger than θ, the error signal is less than zero, and thus NCO decreases $\hat{\theta}(i+1)$. Repeating this procedure, the DOA estimate $\hat{\theta}(i)$ converges to the DOA of the signal θ. When the DOA of the signal is time varying, the DiLL algorithm tracks the DOA of a moving source through iterations.

Note that the negative S-curve slope value ensures that the DOA estimate $\hat{\theta}(i)$ converges to an actual DOA, θ, when the initial DOA estimate is in a certain range which is called a locking range. As shown in Fig. 2, $\theta_{zc,+}$ is the smallest positive value of $\hat{\theta}$, at which the S-curve has a zero value. Similarly, $\theta_{zc,-}$ is the smallest negative value of $\hat{\theta}$, at which the S-curve has a zero value. The locking range for the DiLL is defined as $(\theta_{zc-}, \theta_{zc+})$ in this paper. Since it is difficult to exactly determine $\theta_{zc,+}$ and $\theta_{zc,-}$, $\theta_{zc,+}$ may be approximated as θ_+, which is the smallest positive value of $\hat{\theta}$, at which $|R(\theta, \hat{\theta} - \Delta\theta)|^2$ has a zero value. Similarly, $\theta_{zc,-}$ may be approximated as θ_-, which is the smallest negative value of $\hat{\theta}$, at which $|R(\theta, \hat{\theta} + \Delta\theta)|^2$ has a zero value. From (5), the S-curve is always zero when $\hat{\theta}$ is ±90°. From these results, $\theta_{zc,+}$ and $\theta_{zc,-}$ are approximated as [7]

$$\begin{aligned} \theta_{zc,+} &\approx \min\left(\sin^{-1}\left(\sin(\theta) + \frac{2}{N}\right) + \Delta\theta, 90^\circ\right) \\ \theta_{zc,-} &\approx \max\left(\sin^{-1}\left(\sin(\theta) - \frac{2}{N}\right) - \Delta\theta, -90^\circ\right) \end{aligned}. \tag{8}$$

From (8), it is shown that the locking range is inversely proportional to N, and increases as $\Delta\theta$ increases.

The slope of the S-curve at $\hat{\theta} = \theta$ plays an important role in the DiLL scheme like the DLL scheme [6]. The slope of the S-curve $s(\theta)$ at $\hat{\theta} = \theta$ is calculated as

$$s(q) = \left.\frac{\partial G(\hat{q}(i)|q)}{\partial \hat{q}(i)}\right|_{\hat{q}(i)=q}. \tag{9}$$

Fig. 3 shows the slope of the S-curve as a function of $\Delta\theta$ using (9), when θ=0° and N =8. Note that the slope value oscillates between positive and negative values. It is required for the DiLL scheme to be operated properly that the slope of the S-curve should be negative and the value of $\Delta\theta$ should be chosen as the less one than the first zero crossing point. The $\Delta\theta$ values in Table 1 are what maximize the magnitude of the slope of the S-curve, when θ=0° for N=2,4 and 8.

B. *Characteristics of the modification factor*

In the DiLL scheme, to estimate the DOA of a signal correctly, the value of the S-curve should be zero when $\hat{\theta}(i) = \theta$. When θ=0°, N=4 and $\Delta\theta$=12.24°, the value of the S-curve is zero. This ensures that $\hat{\theta}$ converges to 0° through iterations. However, $G(\hat{\theta}(i) = \theta|\theta)$ is not always zero. Fig. 4 shows the S-curve for θ=60°, N=4 and $\Delta\theta$=12.24°, and indicates that $\hat{\theta}(i)$ does not approach to 60° but to 62.4°. This means that the DiLL scheme is a biased estimator. When $\hat{\theta} = \theta$, $E[e(i)] = G(\theta|\theta)$. It is found from (5) that $G(\theta|\theta)$ may be represented as

$$\begin{aligned} G(\theta|\theta) &= |R(\theta, \theta + \Delta\theta)|^2 - |R(\theta, \theta - \Delta\theta)|^2 \\ &= \frac{4}{N^2}\sum_{n=1}^{N-1}(N-n)\left\{\begin{aligned}&\sin\left(\frac{1}{2}\pi n\begin{pmatrix}(\sin(\theta) - \sin(\theta - \Delta\theta)) \\ -(\sin(\theta + \Delta\theta) - \sin(\theta))\end{pmatrix}\right) \\ &\cdot \sin\left(\frac{1}{2}\pi n(\sin(\theta + \Delta\theta) - \sin(\theta - \Delta\theta))\right)\end{aligned}\right\} \end{aligned}. \tag{10}$$

The term in (10), $(\sin\theta - \sin(\theta - \Delta\theta)) - (\sin(\theta + \Delta\theta) - \sin\theta)$, is not generally zero due to the nonlinearity of the sine function. This is why $G(\theta|\theta)$ is not generally zero. From (10), $G(\theta|\theta)$ is found to increase as $\Delta\theta$ increases.

To remove the bias, the error signal should be modified as follows. For simplification of representation, $G(\theta|\theta)$ is referred to as $m(\theta)$, the modification factor. The modified error signal $e_m(i)$ is represented as

$$e_m(i) = e(i) - m(\theta) = |z_R(i)|^2 - |z_L(i)|^2 - m(\theta). \tag{11}$$

In (11), the actual DOA θ is needed to estimate a modification factor. However, θ is not available in the DOA estimation algorithm. In the DiLL scheme, the DOA estimate $\hat{\theta}$ is used for the modification factor estimation. Thus, the equation (11) may be changed to

$$\hat{e}_m(i) = |z_R(i)|^2 - |z_L(i)|^2 - m(\hat{\theta}) = G_m(\hat{\theta}|\theta) + v_e(i) \tag{12}$$

where $G_m(\hat{\theta}|\theta) \overset{\Delta}{=} G(\hat{\theta}|\theta) - m(\hat{\theta})$, and its characteristic plot is called the modified S-curve. Fig. 4 shows the modified S-curve for $\theta = 60^\circ$. Note that it has a zero value at $\hat{\theta} = 60^\circ$

and has a negative slope value. The DOA estimate at the (i+1)th time may be expressed as

$$\hat{q}(i+1) = \hat{q}(i) + K_0 \cdot (\hat{e}_m(i) \otimes f(i)) \cdot \qquad (13)$$

IV. PERFORMANCE ANALYSIS

In this section, the DOA estimation error variance for the DiLL scheme is analyzed. The DOA estimation error at the ith time $\varepsilon(i)$ may be defined as $\varepsilon(i) \overset{\Delta}{=} \theta - \hat{\theta}(i)$. From (12) and (13), the DOA estimation error at the (i+1)th time may be expressed as

$$\varepsilon(i+1) = \varepsilon(i) - K_0 \cdot \left(G_m\left(\hat{\theta}(i)\middle|\theta\right) + v_e(i)\right) \otimes f(i). \qquad (14)$$

If the DOA estimation error is small enough, $G_m\left(\hat{\theta}(i)\middle|\theta\right)$ may be approximated as $-s_m(\theta)\varepsilon(i)$, where $s_m(\theta) \overset{\Delta}{=} \left.\dfrac{\partial G_m\left(\hat{\theta}(i)\middle|\theta\right)}{\partial\hat{\theta}(i)}\right|_{\hat{\theta}(i)=\theta}$ and $s_m(\theta)$ is a negative value. Thus, the DOA estimation error may be approximated as

$$\varepsilon(i+1) = \varepsilon(i) + K_0 s_m(\theta)\left(\varepsilon(i) - \frac{v_e(i)}{s_m(\theta)}\right) \otimes f(i) \cdot \qquad (15)$$

Thus, the DOA estimation error may be represented in the z-domain as

$$\mathrm{E}(z) = \frac{-K_0 s_m(\theta) F(z) z^{-1}}{1-(1+K_0 s_m(\theta)F(z))z^{-1}} \cdot \left(\frac{V_e(z)}{s_m(\theta)}\right) \qquad (16)$$

where $F(z)$ is the z-transform of the loop filter $f(i)$. Therefore, using (16), the DOA estimation error variance in the steady state, $\sigma^2_{\varepsilon_s}$, may be expressed as [6]

$$\sigma^2_{\varepsilon_s} = \frac{Var(v_e(i))B_L}{s_m^2(\theta)} \qquad (17)$$

where B_L is the two-sided noise bandwidth of the closed loop transfer function, $H(z) \overset{\Delta}{=} \dfrac{-K_0 s_m(\theta)F(z)z^{-1}}{1-(1+K_0 s_m(\theta)F(z))z^{-1}}$. By using (6), the variance of $v_e(i)$ may be expressed as

$$Var(v_e(i)) = \frac{2\sigma^2}{N} \cdot \left(q(\varepsilon_s) - 2\,\mathrm{Re}\left(R(\theta,\theta+\Delta\theta)R^*(\theta,\theta-\Delta\theta)R(\theta+\Delta\theta,\theta-\Delta\theta)\right)\right) \qquad (18)$$

where $q(\varepsilon_s)$ is defined as

$$q(\varepsilon_s) = \left|R(\theta,\theta-\varepsilon_s+\Delta\theta)\right|^2 + \left|R(\theta,\theta-\varepsilon_s-\Delta\theta)\right|^2. \qquad (19)$$

When α and γ are defined as $\alpha = \dfrac{1}{2!} \cdot \left.\dfrac{\partial^2 q(\varepsilon_s)}{\partial {\varepsilon_s}^2}\right|_{\varepsilon_s=0}$ and $\gamma = q(\varepsilon_s)\big|_{\varepsilon_s=0}$, $q(\varepsilon_s)$ may be represented as [6]

$$q(\varepsilon_s) = \alpha\varepsilon_s^2 + \gamma \cdot \qquad (20)$$

Using (17), (18) and (20), $\sigma^2_{\varepsilon_s}$ may be represented as

$$\sigma^2_{\varepsilon_s} = \frac{2\sigma^2 B_L}{N \cdot s_m^2(\theta)} \cdot \left(\alpha\sigma^2_{\varepsilon_s} + \gamma - 2\,\mathrm{Re}\left(R(\theta,\theta+\Delta\theta)R^*(\theta,\theta-\Delta\theta)R(\theta+\Delta\theta,\theta-\Delta\theta)\right)\right) \qquad (21)$$

or solving for $\sigma^2_{\varepsilon_s}$

$$\sigma^2_{\varepsilon_s} = \frac{2B_L}{N \cdot s_m^2(\theta)\cdot\rho} \cdot \frac{\xi}{\left(1-\dfrac{2\alpha \cdot B_L}{N \cdot s_m^2(\theta)\cdot\rho}\right)} \cong \frac{2B_L \cdot \xi}{N \cdot s_m^2(\theta)\cdot\rho} \qquad (22)$$

where $\rho \overset{\Delta}{=} \dfrac{1}{\sigma^2}$ and $\xi \overset{\Delta}{=} \gamma - 2\,\mathrm{Re}\left(R(\theta,\theta+\Delta\theta)R^*(\theta,\theta-\Delta\theta)R(\theta+\Delta\theta,\theta-\Delta\theta)\right)$. When the B_L/ρ is small, $\sigma^2_{\varepsilon_s}$ of the DiLL can be linearly approximated as in (15), thus $\dfrac{2\alpha B_L}{N \cdot s_m^2(\theta)\cdot\rho} << 1$ like the DLL scheme [6]. Since the signal power is assumed to be 1 and the noise variance is σ^2 for each antenna element, as described in Section II, ρ represents the signal-to-noise (SNR). From (22), $\sigma^2_{\varepsilon_s}$ is inversely proportional to SNR.

V. NUMERICAL RESULTS

In this section, the analysis and simulation results for the DOA estimation error variance, $\sigma^2_{\varepsilon_s}$ are shown to compare the performance of the DiLL and PASTd based DOA estimation algorithm. A uniform linear array of omni-directional antenna elements with half-wavelength spacing is used for analysis and simulation. Analysis and simulation are performed for a single user case. The parameters used in the analysis and simulation are selected to make the DOA estimation error variances for both scheme be equal with SNR=10dB, θ=18°. For the DiLL scheme, the NCO gain K_0 is set equal to 0.05, and the one-pole IIR filter with forgetting factor 0.9 is used for the loop filter whose z-transform is $F(z) = \dfrac{0.1}{1-0.9z^{-1}}$. The values in Table 1 are used for $\Delta\theta$ regardless of the DOA of a signal. They maximize the absolute value of the slope in the S-curve for each N. For the PASTd, the forgetting factor is set equal to 0.97 and the initial value of the eigenvalue estimate is chosen to be one [5]. After each subspace update, ESPRIT [3] is applied to compute the DOA of signals from the signal subspace estimate [4], [5].

A. DOA estimation accuracy vs. DOA of signal q

Fig. 5 shows how $\sigma^2_{\varepsilon_s}$ for the DiLL scheme varies with the DOA of a signal for N=2, 4, and 8, when SNR is 10dB. In this figure, the simulation results for the DiLL with an unmodified error signal and the PASTd with ESPRIT are also shown when N =8. Note that the simulation and analytical results for the DiLL scheme are very close. $\sigma^2_{\varepsilon_s}$ for the DiLL scheme using a modified error signal is found to be relatively insensitive to θ in comparison with those for the DiLL using an unmodified error signal, and the PASTd with ESPRIT. Thus, the DOA estimation accuracy of the DiLL becomes better than that of the PASTd with ESPRIT as the magnitude of θ increases.

B. DOA tracking for a moving source

In this subsection, the tracking performance of the DiLL scheme is investigated when N=8, SNR=10dB, and the parameters are same as the previous simulation. Fig. 6 shows the trajectories and the tracking error of the DiLL scheme and PASTd with ESPRIT. Fig. 6 (a) shows the true trajectory of a DOA over time, and the trajectories tracked using the DiLL scheme and the PASTd with ESPRIT. The DOA $\theta(i)$ stays at 18° for the first 100 symbol period, and then the DOA of a signal varies as $\theta(i) = \left[-60\sin\left(\dfrac{i-100}{1000}\right)+18\right]^\circ$ from the 100th to the 4000th symbol time. Fig. 6 (b) shows for the two scheme the squares of the DOA tracking error, obtained by ensemble averaging over 100 independent trials. For the PASTd with

ESPRIT scheme, when the DOA of a signal start to change at the 100th symbol time, the DOA tracking error increases significantly, and then, the DOA tracking error decreases as the rate of the DOA angle change decreases. The DOA tracking error again increases, as the rate of DOA angle change increases. Unlike the PASTd with ESPRIT, the DiLL scheme is relatively insensitive to the variation in the rate of DOA angle change. The reason is that if B_L is larger than the rate of DOA angle change, the tracking error is only related with the noise variance. Thus, the tracking error is insensitive to the rate of DOA angle change.

From these results, it is found that the DiLL scheme has the better tracking capability than the PASTd with ESPRIT when the two schemes have the same DOA estimation error variance.

VI. CONCLUSIONS

In this paper, a DOA estimation algorithm, DiLL is proposed and analyzed. It estimates the DOA of a signal iteratively by using the difference of the correlation of an input signal and the array response vectors whose directions are $\pm\Delta\theta$ shifted from the DOA estimate.

The DiLL scheme is found to track better than the PASTd based DOA estimation scheme, and its performance is less sensitive to the DOA of a signal than that of the PASTd based DOA estimation scheme when the two scheme have the same DOA estimation error variance.

REFERENCES

[1] L. C. Godara, "Applications of Antenna Arrays to Mobile Communications, Part II: Beam-Forming and Direction-of-Arrival Considerations," *Proc. IEEE*, vol. 85, no. 8, pp. 1195-1245, Aug. 1997.

[2] R. O. Schmidt, "Multiple Emitter Location and Signal Parameter Estimation," *IEEE Trans. Antennas Propagat.*, vol. 34, no. 3, pp. 276-280, Mar. 1986.

[3] R. Roy and T. Kailath, "ESPRIT-Estimation of Signal Parameters via Rotational Invariance Techniques," *IEEE Trans. Acoust., Speech, Signal Processing*, vol. 37, no. 7, pp. 984-995, Jul. 1989.

[4] B. Yang, "Projection Approximation Subspace Tracking," *IEEE Trans. Signal Processing*, vol. 43, no. 1, pp. 95-107, Jan. 1995.

[5] B. Yang, "An Extension of the PASTd Algorithm to Both Rank and Subspace Tracking," *IEEE Trans. Signal Processing*, vol. 43, no. 9, pp. 179-182, Sep. 1995.

[6] M. K. Simon, "Noncoherent pseudonoise code tracking performance of spread spectrum receivers," *IEEE Trans. Commun.*, vol. 25, no. 3, pp. 327-345, Mar. 1977

[7] R. A. Monzingo and T. W. Miller, *Introduction to Adaptive Arrays*, 1980.

[8] B. D. Rao and K. V. S. Hari, "Performance Analysis of ESPRIT and TAM in Determining the Direction of Arrival of Plane Waves in Noise," *IEEE Trans. Acoust., Speech, Signal Processing*, vol. 37, no. 12, pp. 1990-1995, Dec. 1989.

Table 1. $\Delta\theta$

	$\Delta\theta$ (degrees)
N=2	26.28°
N=4	12.24°
N=8	6.12°

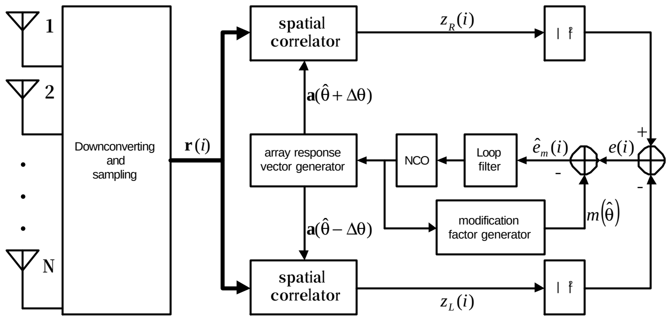

Fig.1. Block diagram of the DiLL scheme

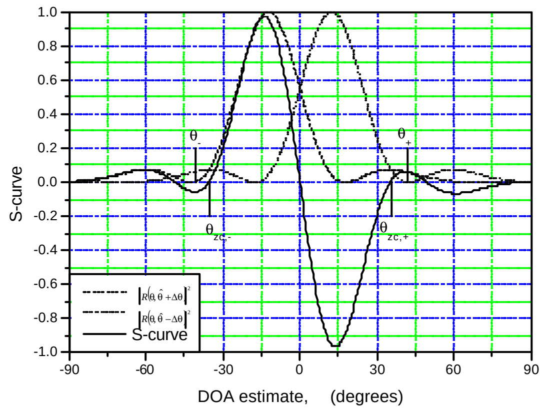

Fig. 2. S-curve (θ=0°, N=4, $\Delta\theta$=12.24°)

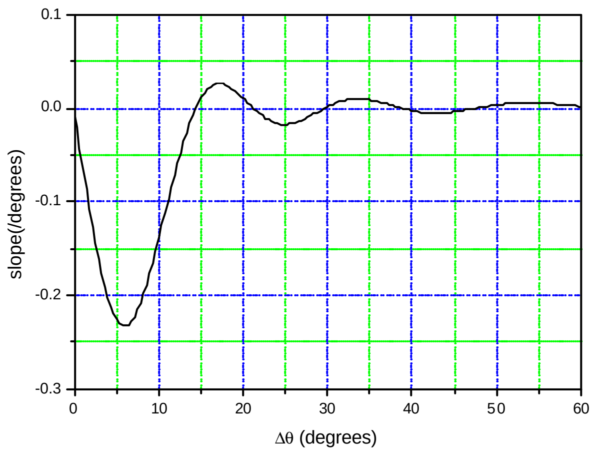

Fig. 3. The slope of the S-curve (θ=0°, N=8)

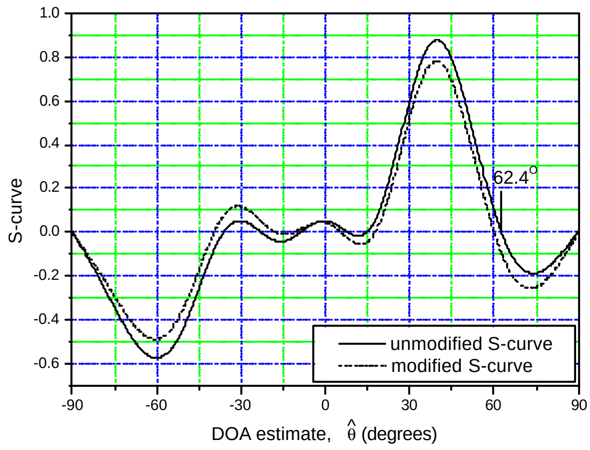

Fig. 4. Modified and Unmodified S-curves
(θ=60°, N=4, $\Delta\theta$=12.24°)

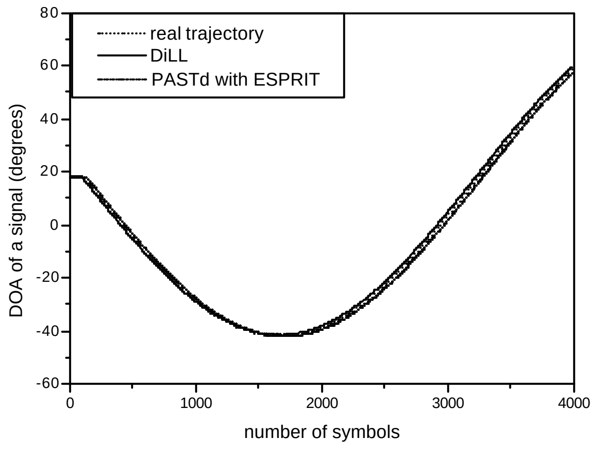

(a)

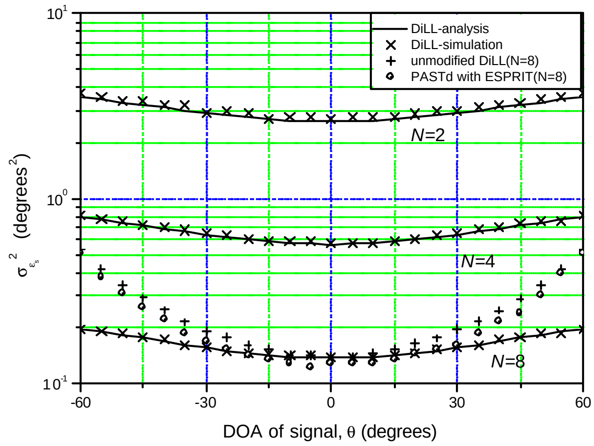

Fig. 5. DOA estimation error variance

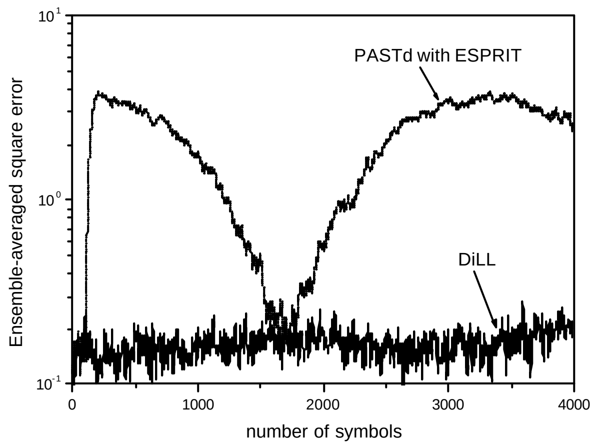

(b)

Fig. 6. DOA tracking of the time-varying $\theta(i)$